CHEMISTRY
A EUROPEAN JOURNAL

DOI: 10.1002/chem.200601246

Synthesis, Structure, and Characterization of Three Series of 3d–4f Metal-Organic Frameworks Based on Rod-Shaped and (6,3)-Sheet Metal Carboxylate Substructures

Feng Luo,[a] Stuart R. Batten,[b] Yunxia Che,[a] and Ji-Min Zheng*[a]

Abstract: Three series of porous lanthanide metal-organic coordination polymers, namely $[Cu(bpy)Ln_3(ip)_5(Hip)(H_2O)]$ [Ln = Er (**1a**), Y (**1b**), Eu (**1c**); bpy = 2,2′-bipyridine, H_2ip = isophthalic acid], $[Cu_3(bpy)_2Ln_2(ip)_6(H_2O)_5]$ [Ln = Yb (**2a**), Gd (**2b**), Tb (**2c**)], and $[Cu_3Ln_2(ip)_6]$ [Ln = Eu (**3a**), Gd (**3b**)] have been synthesized hydrothermally by the reaction of the combination of 3d–4f metal centers and N-/O-donor ligands. X-ray diffraction analyses reveal that polymers **1a–c** and **2a–c**, as well as **3a**,**b** are isomorphous in structure. Polymers **1a–c** consist of 3D α-Po networks based on a inorganic rod-shaped secondary building units (SBUs) of $\{Er_6Cu_2(bipy)_2(O_2C)_{11}\}$ which are 27.03 Å in length. Polymers **2a–c** also contain 3D α-Po networks, constructed from shorter (14.79 Å) but similarly rod-shaped SBUs of $\{Yb_2Cu_3(bpy)_2(O_2C)_{12}\}$. The structure also contains hydrogen-bonded $(H_2O)_6$ chains which can be reversibly dehydrated/rehydrated. Polymers **3a**,**b** contain metal carboxylate substructures which have 2D (6,3) topologies; these layers are bridged by the ip^{2-} ligands to give an overall 3D network which contains two sorts of cavities. This series of Ln–Cu coordination polymers are further characterized by antiferromagnetic behavior.

Keywords: coordination modes · lanthanides · open frameworks · polymers · porous materials

Introduction

There has been growing interest in recent years in the design and synthesis of heterometallic complexes, such as 3d–4f or 4d–4f polymeric metal systems, motivated by their fascinating structural topology and the exploitable applications in magnetism, luminescent materials, molecular adsorption and bimetallic catalysis.[1] In a recent review by Shore and co-workers, existing Ln–M coordination polymers were summarized and a rational classification was proposed according to the different types of interactions between Ln–M: 1) Ln–M direct bonds, 2) ionic associations, 3) Ln–linkers–M.[1] For the Ln–linkers–M system in particular a large number of examples have been assembled from aggregation of Ln–M hetrometallic ions and diverse N-/O-donor ligands, which not only have attractive topologies but also interesting magnetic and luminescent behavior.[2] To target Ln–M coordination polymers by design, a reasonable choice of ligands is important. In general, multidentate ligands containing both N- and O-donor atoms are usually employed in the construction of Ln–M coordination polymers, in keeping with the typical coordination behaviors of Ln and M ions. For example, Hong and co-workers pioneered the study of the assembly of the suitable pyridine carboxylate ligands containing both N- and O-donor (such as pyridine-2,5-dicarboxylic acid, pyrazine-2,4-dicarboxylic acid and several amino acids) with lanthanide and transition metal ions, and isolated a series of Ln–M coordination polymers with intriguing structural motifs, magnetic and luminescent properties. Yang and co-workers employed the rigid isonicotinic acid to construct the consecutive multinuclear $Ln_{14}Cu_6$ polymers.[3]

Further research, however, is needed in this area. Thus, we report herein the investigations of the assembly of mixed 2,2′-bipyridine (bpy) (N-donor) and isophthalic acid (H_2ip) (O-donor) ligands with Ln–Cu heterometallic ions as another route to Ln–Cu polymers.

[a] Dr. F. Luo, Prof. Y. Che, Prof. J.-M. Zheng
Department of Chemistry, Nankai University
Tianjin 300071 (China)
Fax: (+86) 22-2350-8056
E-mail: jmzheng@nankai.edu.cn

[b] Dr. S. R. Batten
School of Chemistry, P.O. Box 23, Monash University
Clayton, Victoria 3800 (Australia)

Supporting information for this article is available on the WWW under http://www.chemeurj.org/ or from the author: TG plots, XRD patterns and $\chi_M T$ vs T plots of these polymers.

Results and Discussion

Description of structures: Single-crystal X-ray diffraction (XRD) analysis reveals that polymers **1a–c**, **2a–c** and **3a**,**b** are isomorphous. Thus, only the representative complexes **1a**, **2a**, and **3a** are discussed in more detail.

Crystal structure of complex 1a: The asymmetric unit of $[Cu(bpy)Er_3(ip)_5(Hip)]\cdot H_2O$ (**1a**) contains one $Cu(bpy)^{2+}$ moiety, three Er^{III} ions, five ip^{2-} ions, one Hip^- ion, and one intercalated water molecule. The Cu^{2+} atom is five-coordinate and coordinated to one bpy ligand and three ip^{2-} ligands, with pyramidal CuO_3N_2 geometry (the metal atom is displaced from the plane defined by N1, N2, O4 and O11 by 0.275 Å). The Er1 atom has eight-coordinated, distorted bicapped trigonal prismatic geometry and coordinates to one Hip^- and five ip^{2-} ligands. The Er3 and Er2 atoms both have seven-coordinated, monocapped trigonal prismatic geometries, coordinating to six ip^{2-} ligands, or one Hip^-/six ip^{2-} ligands, respectively. The Er–O bond lengths (Table 2) range from 2.223(4) to 2.492(3) Å. The ip^{2-} and Hip^- ligands in turn show a variety of bonding modes, with ip^{2-} adopting a range of tetradentate modes, and Hip^- bidentate, as shown in Figure 1.

The ligands bridge the metal atoms into a complicated 3D network that can be simplified by considering the metal carboxylate substructure. Long 27.03 Å octanuclear "rods" are formed which are composed of chains of six Er^{III} atoms terminated at either end by Cu^{II}(bpy) groups. The rods lie across inversion centers, relating one half to the other, and the metals are bridged by carboxylate groups and μ_2-$O_{carboxylate}$ atoms to give the Er-O-C-O-Er, Er-O-C-O-Cu, Er-O-Er, and Er-O-Cu linkages (Figure 2). The metal carboxylate $Er_6Cu_2(bpy)_2(O_2C)_{11}$ moieties can be considered as secondary building units (SBUs), with each rod connected to six others via the ip^{2-} bridges (four rods are connected by four bridges each, while the other two are connected by pairs of ip^{2-} bridges). Thus the SBUs act as six-connecting nodes, and a 3D α-Po network is formed (Figure 3).

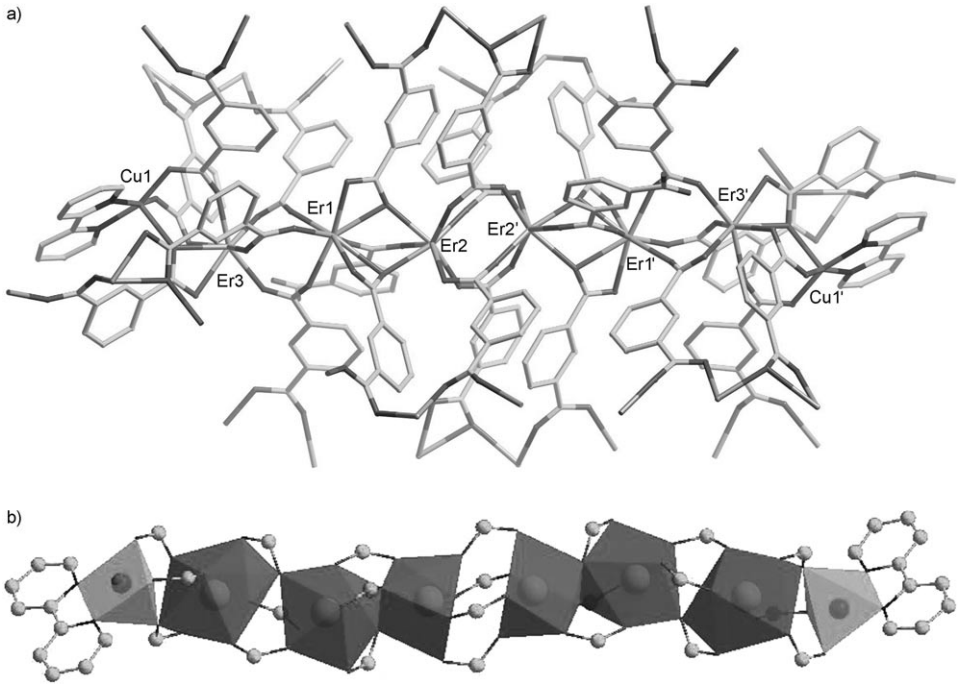

Figure 2. a) View of the rod-shaped $\{Er_6Cu_2(bpy)_2(O_2C)_{11}\}$ SBU in the structure of **1a**. b) Polyhedral representations of the rod-shaped $\{Er_6Cu_2(bpy)_2(O_2C)_{11}\}$ SBU.

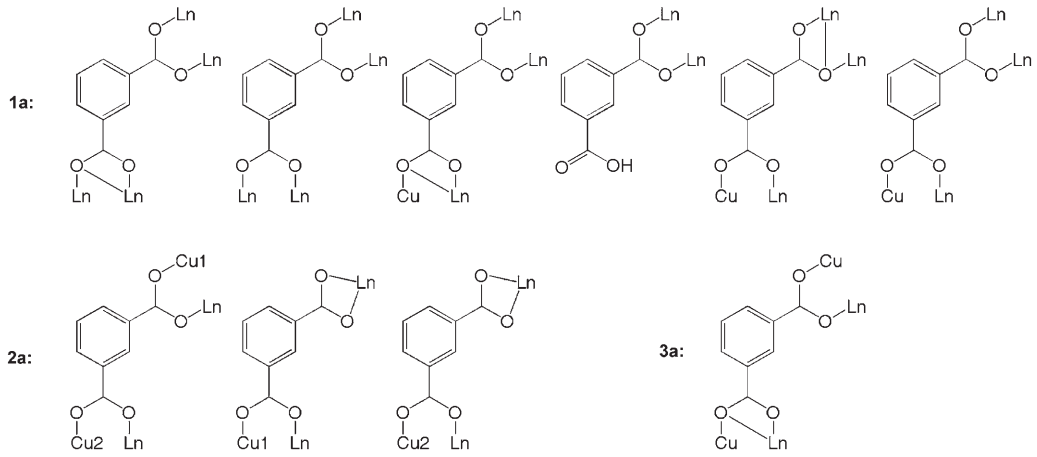

Figure 1. Schematic description of the coordinated modes for Hip^-/ip^{2-} ligands in **1a–c**, **2a–c**, **3a**,**b**.

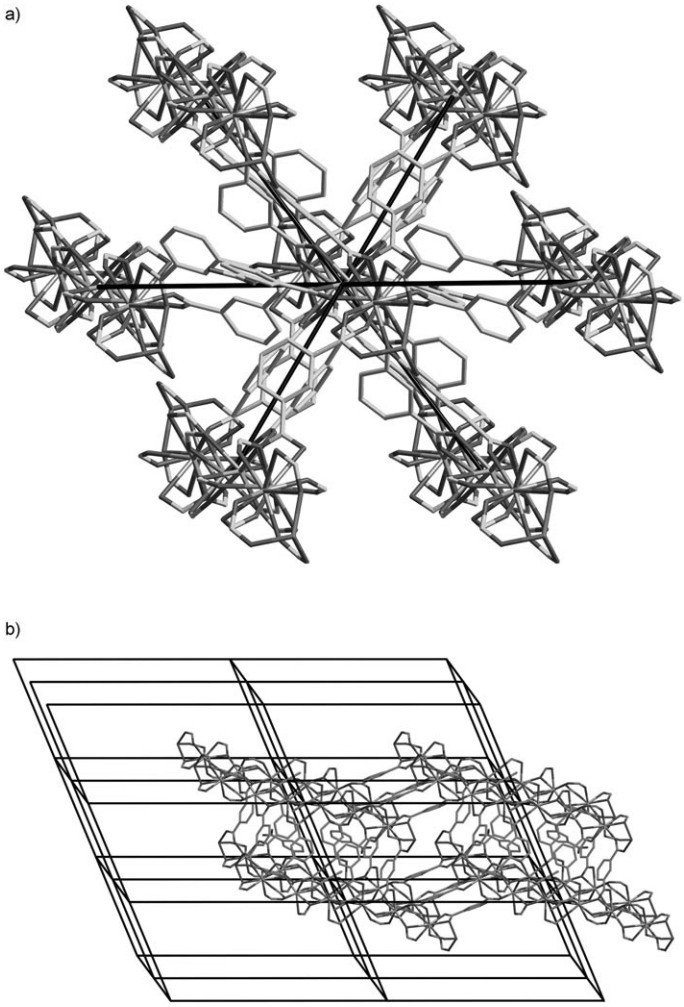

Figure 3. a) View of the connection of one $\{Er_6Cu_2(bpy)_2(O_2C)_{11}\}$ SBU to six others in **1a**; the black lines represent the connections schematically by connecting the centres of each SBU. b) A view of the overall 3D α-Po network, with one "cube" of eight SBUs shown in full, and the network expanded further in a schematic fashion.

The long rod-shaped SBUs are unique and very different to other reported metal carboxylate SBUs, which include $M_2(O_2C)_3$, $M_2(O_2C)_4$, $M_3O(O_2C)_6$ and $M_4O(O_2C)_6$ globular cluster topologies.[4] One rod-shaped SBU has been reported: the structure of $[Zn_3(bdc)_3]\cdot 6MeOH$ (BDC = benzene-1,4-dicarboxylate) contains trimeric $Zn_3(O_2C)_6$ clusters acting as six-connecting SBUs; an α-Po network is also formed.[5]

Crystal structure of complex 2a: The structure of $[Cu_3(bpy)_2Yb_2(ip)_6]\cdot 5H_2O$ (**2a**) is similarly complicated, with the asymmetric unit containing two unique Cu^{II} atoms (one of which (Cu2) lies on an inversion center), one Yb atom, one bpy ligand, three ip^{2-} ligands and five intercalated water molecules. The copper atoms have square planar geometries, with Cu1 coordinated to one bpy chelate and two carboxylate anions (ignoring the weak Cu1–O7 interaction (2.675 Å); the corresponding distances in **2b** and **c** are 2.982 and 2.819 Å, respectively). Cu1 lies 0.206 Å out of the plane of the donor atoms (0.172 and 0.182 Å, respectively, for **2b** and **c**). The Cu2 atom coordinates to four ip^{2-} ligands. The Yb atom coordinates to six ip^{2-} ligands with eight-coordinated, distorted bicapped trigonal prismatic geometry. The three different ip^{2-} ligands show two distinct coordination modes (Figure 1). The Yb–O bond lengths range from 2.228 to2.445 Å (Table 2).

Like **1a**, the carboxylate ligands bridge the metal atoms into rod-shaped motifs (Figure 4). In this case, the rods are pentanuclear, containing three Cu atoms and two Yb atoms. As before, the ends are terminated by $Cu(bpy)^{2+}$ moieties (Cu···Cu 14.79 Å), and the rods lie across inversion centers (upon which the central Cu2 ion lies). Remarkably, as for the octanuclear SBUs in **1a**, the pentanuclear $Yb_2Cu_3(bpy)_2(O_2C)_{12}$ SBUs in **2a** are each connected to six others (by pairs of ip^{2-} ligands; Figure 5) to again generate the six-connected α-Po network.

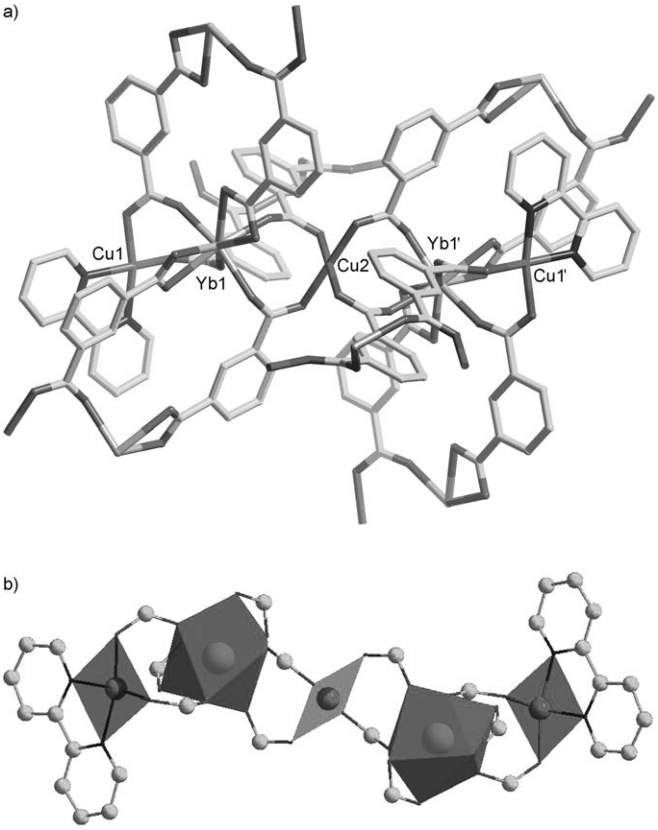

Figure 4. a) View of the rod-shaped $\{Yb_2Cu_3(bpy)_2(O_2C)_{12}\}$ SBU in the structure of **2a**. b) Polyhedral representations of the rod-shaped $\{Yb_2Cu_3(bpy)_2(O_2C)_{12}\}$ SBU.

Another interesting feature of **2a** are the 1D channels with approximate dimensions 10.7×13.3 Å. These channels contain hydrogen bonded $(H_2O)_6$ chains (O13–O14 2.853, O13–O15 2.728, O15–O15A 2.986 Å) and the larger Cu(bpy) fragments (Figure 6).

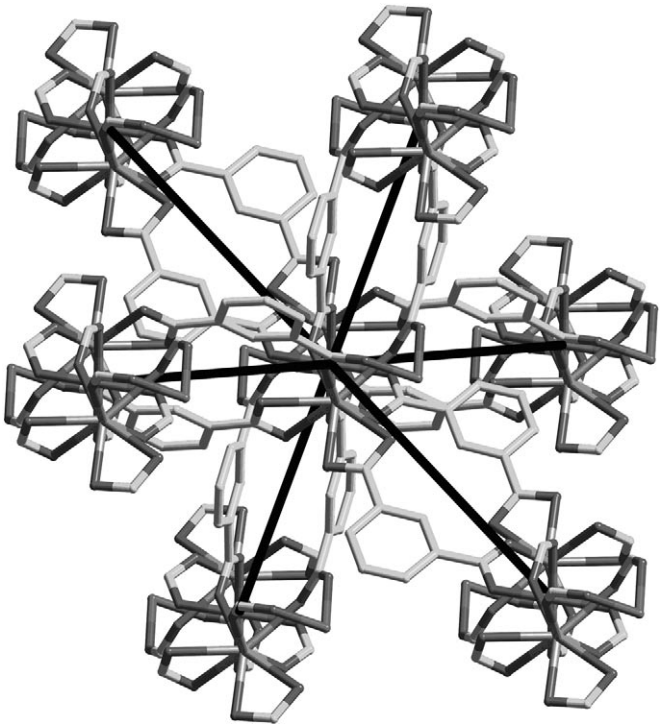

Figure 5. View of the connection of one $\{Yb_2Cu_3(bpy)_2(O_2C)_{12}\}$ SBU to six others in **2a**; the black lines represent the connections schematically by connecting the centres of each SBU.

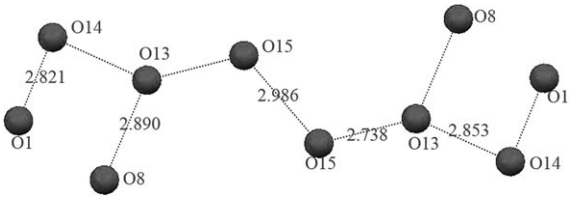

Figure 6. Chain-like $(H_2O)_6$ molecules linked by typical hydrogen bonds and ligated to the 1D channel through O13–O8/O13A–O8A, O14–O1/O14A–O1A hydrogen bonds.

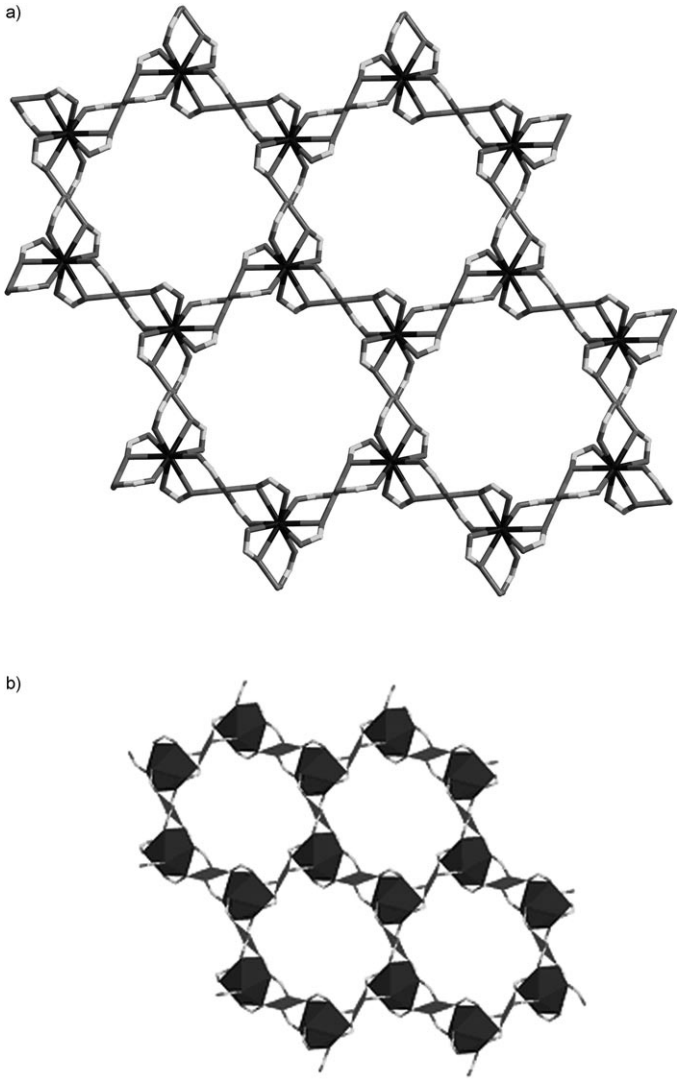

Figure 7. a) View of the 2D (6,3)-sheet substructure in **3a** formed by the bridging of the metal ions by the ligand carboxylate groups. b) Polyhedral representations of the 2D (6,3)-sheet substructure.

Crystal structure of complex 3a: The structure of $[Cu_3Eu_2(ip)_6]$ (**3a**) is less complicated than the two previous structures in that it contains only one type of Cu atom, one unique Eu atom, and one unique ip^{2-} ligand. The Cu atom is coordinated to four ip^{2-} ligands in a square-planar arrangement, while the Eu atoms are coordinated to six ip^{2-} ligands in an nine-coordinate distorted tricapped trigonal prismatic fashion. The ip^{2-} ligand shows a tetradentane bridging mode to link Eu and Cu atoms in the Eu-O-C-O-Cu and Eu-O-Cu fashions (Figure 1.) Despite the simple asymmetric unit, the structure is nonetheless complicated, due to the high symmetry (rhombohedral space group $R\bar{3}c$). Examination of the metal carboxylate substructure reveals that, unlike **1a** and **2a**, a 2D hexagonal network is formed rather than discrete rods, with Eu centers acting as nodes (Eu···Eu 7.60 Å), and Cu atoms lying midway along an edge (Figure 7). These layers stack in an ABC fashion, and are connected by the ip^{2-} pillars into an overall 3D network (Figure 8). Two different cavities are created, as shown in Figure 9. The smaller cavity (Figure 9a) lies between two adjoining sheets and is composed of two $EuCu_3$ groups bridged by six ip^{2-} pillars (Eu···Eu 8.45 Å). The larger cavity (Figure 9b) also contains six ip^{2-} pillars, but is defined by the hexagonal window of one sheet capped above and below by Eu nodes of the adjoining sheets, and thus spans across three sheets. The Eu···Eu distance from sheet 1 to sheet 3 is 15.02 Å, while the Eu···Eu diameter across the hexagonal window of sheet 2 is 15.15 Å.

From the structures of the three series of 3d–4f polymers reported here, it is obvious that the bpy ligands play an important template role in the formation of these products: i) if the Cu/bpy ratio is 1:1, polymers **1a–c** will be the products, in which each Cu^{II} atom is ligated by one bpy ligands; ii) when the Cu/bpy ratio is 2:1, polymers **2a–c** are the only

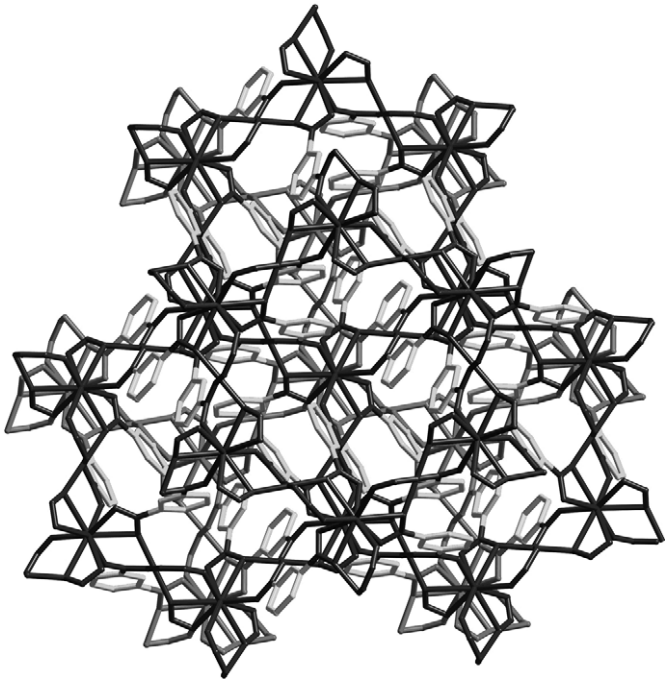

Figure 8. View of three (6,3) metal carboxylate layers in **3a** connected by the bridging ip^{2-} pillars, to form a 3D network. For clarity, the metal ions and CO_2^- groups of each layer are shaded differently.

products with only one half of Cu^{II} atoms coordinated by bpy ligands; iii) if the bpy ligands are removed, obviously different polymers **3a**,**b** are obtained.

As mentioned above, in polymers **1a–c**, the ip^{2-} ligands adopt six-coordinated modes, especially the tridentate bridge from one carboxylate group, that is the key factor for the formation of the high metal nuclearity (octanuclear), rather than the pentanuclear in polymers **2a–c**. Interestingly, through self-assembly, the two different SBUs (octanuclear, and pentanuclear) would like to give rise to the same structure(α-Po nets).

However, in the three series of porous lanthanide metal-organic coordination polymers, the average bridging Ln–O bond lengths mainly show a regular order: upon the increasing atomic number, the average bridging Ln–O bond lengths will gradually decrease; the reason may be the lanthanide contraction.

Magnetic properties: The temperature-dependent magnetic susceptibility data of compounds **1a**,**c**, **2a–c** and **3a**,**b** were measured for crystal samples at an applied magnetic field of 1000–500 Oe in the temperature range of 5-/or 2–300 K. The plots of $\chi_M T$ versus T of these compounds are shown in Figure 10 and Supporting Information.

As illustrated in these plots of $\chi_M T$ versus T, the observed $\chi_M T$ value for each compound is very close to the theoretical value at room temperature, expected for a coupling-free system of isolated Ln^{III} and Cu^{II} ions, which confirms the assignment of oxidation states as judged by the neutrality requirement (in polymers **1c** and **3a**, the Eu^{III} ions with lower

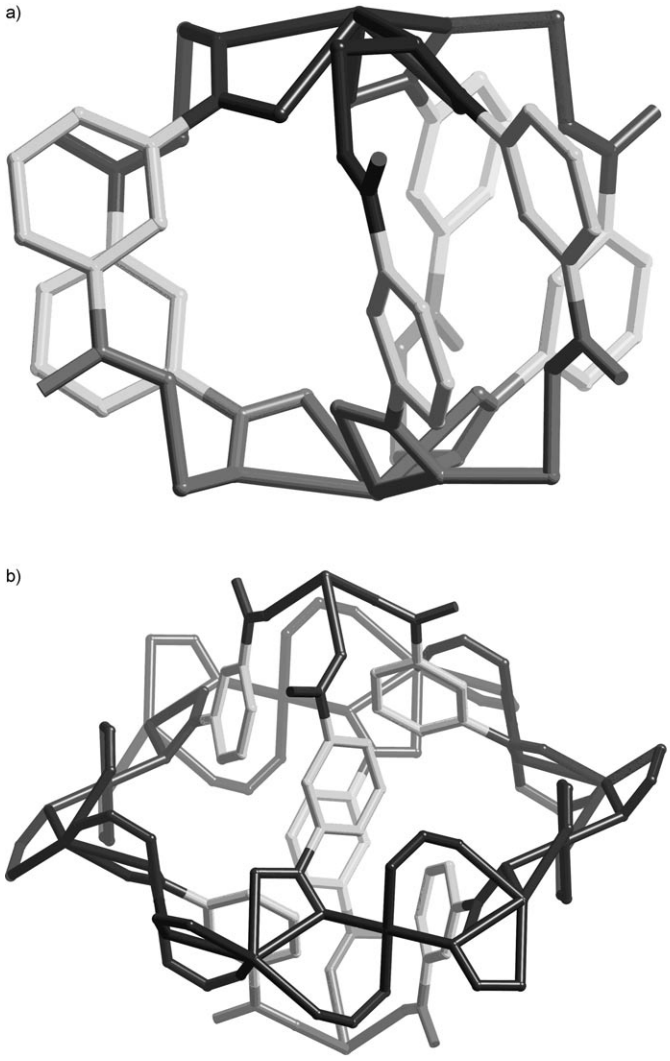

Figure 9. Views of a) the smaller cavity and b) the larger cavity in the structure of **3a**.

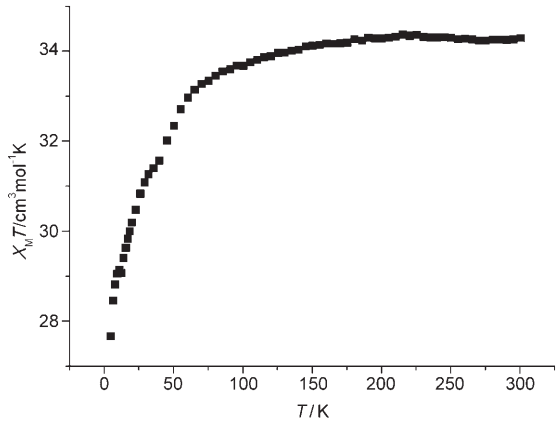

Figure 10. Plot of $\chi_M T$ vs T for polymer **1a**.

excited state of ^7F_J are considered; at low temperature, the Eu^{III} ions own the $J=0$ ground state ($^7F_0$)).[6] Upon the cooling temperature, the corrected $\chi_M T$ value decreases for all

compounds. The nature of such antiferromagnetic-like behavior remains to be clarified for 4f–3d compounds, but it may be related to the progressive thermal depopulation of the Ln^{III} Stark components and a possible the Ln^{III}–Cu^{II} interaction. Because of the large separation between the Ln^{III} ions and the well-shielded 4f orbitals by the outer shells of 5s and 5p orbitals as well as relatively low covalence of the lanthanide-to-ligand bonds, the Ln–Ln interactions are expected to be negligibly small.[7]

Thermogravity (TG) and powder X-ray diffraction analysis: Due to the structural similarities of all the compounds, only polymers **1a**, **2a**, and **3a** were studied by using TG analysis to confirm the thermal stability of the present framework structure (see Supporting Information). In particular, for polymer **2a**, a combination of IR, TG and corresponding powder X-ray diffraction analysis was undertaken to evaluate the reversibility of dehydration and rehydration of the chain-like $(H_2O)_6$ molecules.

The thermal stability of **1a** has been studied by TG. The TG, performed from 30 to 600 °C with ratio of 10 °C min^{-1}, shows that the first weight loss of 1.2% from 80 to 120 °C, corresponds to the loss of the one free water molecule (calcd for 1.22%). The decomposition of complex starts about 420 °C.

Under the same conditions, the TG of polymer **2a** showed two major weight loss: the first weight loss of 5.3% from 80 to 100 °C corresponds to the loss of the free water molecules (calcd for 4.7% for $[H_2O]_{2.5}$), and the second was due to chemical decomposition after 400 °C. According to the IR bands at 3467 cm^{-1}, the encapsulated water molecules can be ascribed to the liquid water.[2] The powder XRD studies were performed on the crystal samples and heated at 30 and 150 °C. Comparing the powder XRD patterns of **2a** at 150 °C with those of the samples at 30 °C, we found that the departure of the guest molecules does not lead to any phase transformation. However, the existence of guest molecules in this framework and the thermal stability encouraged us to remove the guest molecules and try to create the micropores (if the capsulated water molecules are removed, the volume of the cavities will be up to 215.2 Å^3 per unit cell, or 12.8% of the cell volume, centered on the position (0.500, 0.500 0.000)).[9] Thus we performed the following additional experiments: i) dehydration: the crystal samples of **2a** were heated at 150 °C until there was no more weight loss, and in order to confirm the full weight loss of guest molecules, IR and powder XRD were measured (IR without the 3467 cm^{-1} band, XRD pattern without the water peak), and the result shows that the process of dehydration was completed; ii) rehydration: the dehydrated sample was exposed to water vapor for about 24 h, and then IR and powder XRD measurements were repeated (IR with the 3467 cm^{-1} band, XRD pattern with the water peak), which suggested that the rehydration had been completed (Figure 11).

For polymer **3a**, there exist no guest molecules in the permanent, hydrophobic microvoids, which is consistent with the TG analysis: at 30–400 °C, there is no weight loss, and decomposition occurs after 400 °C.

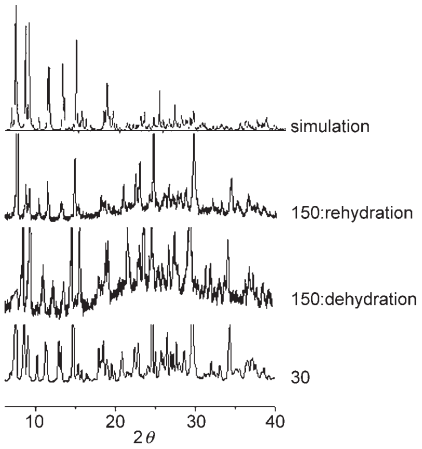

Figure 11. Designed powder XRD plot of **2a**: comparison of the XRD plot at 30, 150 °C (dehydration) and the simulation pattern with the rehydrated pattern; it is believed that the structure can be reversibly dehydrated and rehydrated.

Conclusion

Three series of 3D 3d–4f frameworks have been synthesized hydrothermally, based on the assembly of mixed 2,2′-bipyridine (bpy) (N-donor) and isophthalic acid (H_2ip) (O-donor) ligands with Ln–Cu heterometallic ions. Topological analyses of the three series of complexes indicate that polymers **1a–c** and **2a–c** feature the same topology (α-Po nets) constructed from different rod-shaped SBUs, and polymers **3a**,**b** are characterized by the 2D (6,3) nets pillared by ip^{2-} ligands. In addition, some other properties, such as the hydrogen bonded $(H_2O)_6$ chains which can be reversibly dehydrated/rehydrated, as well as the pillared (6,3) nets with two sorts of cavities, are also attractive for the potential application as porous materials.[11] The investigations of the magnetic behavior of this system deserve further attention not only for the fundamental nature of Ln–Cu complexes but also for understanding the chemistry of such compounds already in use and for future applications. It is believed that the preliminary results presented here may also provide a promising pathway to rational design of diversely 3d–4f frameworks, a goal that we are pursuing actively.

Experimental Section

Materials and instruments: All reagents were bought from commercial sources without further purification. IR (KBr pellets) spectra were recorded in the 400–4000 cm^{-1} range using a Perkin–Elmer Spectrum One FTIR spectrometer. The elemental analysis was carried out on Elementar Vario ELIII microanalyzer; TG analysis was performed with a heating rate of 10 °C min^{-1} using a Netzsch STA 449C simultaneous TG-DSC instrument. Magnetic measurements were carried out with a Quantum Design (SQUID) magnetometer MPMS-XL-5.

Synthesis of 1a–c: An aqueous mixture (10 mL) of Ln_2O_3, $Cu(NO_3)_2$, ip and bpy in the ratio of 1:2:1:2 was placed in a Teflon reactor (23 mL), and heated at 170 °C for 5 d, and then it was cooled to room temperature at 5 °C h^{-1}. Green crystals were obtained in 70 (**1a**), 76 (**1b**), 68% (**1c**) yield based on Cu. In addition, $Ln(NO_3)_3$ or $LnCl_3$ was used instead of Ln_2O_3 to produce **1a–c**, without obviously change in the yield; on the other hand, $CuCl_2$ or $CuSO_4$ was also selected to replace $Cu(NO_3)_2$ to produce polymer **1a–c**, without obviously change in the yield. The phase purity of the bulk materials of **1a** was corroborated by powder X-ray diffraction study (see Figure S5, Supporting Information) and elemental analysis. Elemental analysis calcd (%) for **1a**: C 40.59, H 2.00, N 1.63; found: C 40.28, H 1.89, N 1.73; IR (KBr): $\tilde{\nu}$ = 3466(m), 3066(m), 1728(s), 1631(m), 1604(m), 1471(w), 1453(s), 1408(m), 1275(m), 1175(s), 1116(s), 1019(m), 927(s), 830(s), 714(s), 630(m), 435(m) cm^{-1}.

Synthesis of 2a–c: An aqueous mixture (10 mL) of Ln_2O_3, $Cu(NO_3)_2$, ip and bpy in the ratio of 1:2:1:1 was placed in a Teflon reactor (23 mL), and heated at 170 °C for 5 d, and then it was cooled to room temperature at 5 °C h^{-1}. Blue crystals were obtained in 73 (**2a**), 66 (**2b**), 68% (**2c**) yield based on Cu. In addition, $Ln(NO_3)_3$/$LnCl_3$ and $CuCl_2$/$CuSO_4$ were selected to replace Ln_2O_3 and $Cu(NO_3)_2$ to produce polymer **2a–c**, and the yield is not obviously changed. The phase purity of the bulk materials of **2a** was corroborated by powder X-ray diffraction study (see Figure 11) and elemental analysis. Elemental analysis calcd (%) for **2a**: C 42.45, H 2.62, N 2.91; found: C 43.08, H 2.49, N 2.93; IR (KBr): $\tilde{\nu}$ = 3467(m), 3118(m), 1630(m), 1606(m), 1479(w), 1448(s), 1403(m), 1278(m), 1176(s), 1107(s), 1035(m), 939(s), 835(s), 750(s), 725(s), 660(m), 479(m) cm^{-1}.

Synthesis of 3a,b: An aqueous mixture (10 mL) of Ln_2O_3, $Cu(NO_3)_2$, ip in the ratio of 1:2:1 was placed in a Teflon reactor (23 mL), and heated at 170 °C for 5 d, and then it was cooled to room temperature at 5 °C h^{-1}. Blue crystals were obtained in 53 (**3a**), 46% (**3b**) yield based on Cu. To our surprise, in this system, if Ln_2O_3 and $Cu(NO_3)_2$ were replaced by $Ln(NO_3)_3$/$LnCl_3$ and $CuCl_2$/$CuSO_4$. The phase purity of the bulk materials of **3a** was corroborated by powder X-ray diffraction study (see Figure S6, Supporting Information) and elemental analysis. Elemental analysis calcd (%) for **3a**: C 39.05, H 1.64; found: C 38.98, H 1.71; IR (KBr): $\tilde{\nu}$ = 3674(s), 3066(s), 2368(m), 1961(m), 1918(m), 1874(m), 1767(m), 1599(m), 1546(m), 1476(w), 1448(s), 1413(m), 1362(s), 1276(m), 1179(s), 1104(s), 1078(m), 936(s), 841(s), 806(m), 743(s), 728(s), 662(m), 601(s), 566(s), 479(m) cm^{-1}.

X-ray crystallography: Intensity data were collected on a Bruker SMART 1000 CCD bidimensional detector with $Mo_{K\alpha}$ monochromated radiation (λ = 0.71073 Å) at room temperature. Empirical absorption correction was applied. The structures of these polymers were solved by the direct method and refined by the full-matrix least squares on F^2 using the SHELXL-97 software.[10] All of the non-hydrogen atoms were refined anisotropically. The organic hydrogen atoms were generated geometrically; the aqua hydrogen atoms were located from difference maps and refined with isotropic temperature factors. Crystal data and structure refinement for these polymers are summarized in Table 1. Selected bond lengths and angels are listed in Table 2.

CCDC-285866–285864 for **1a–c**, -286703–286705 for **2b**,**a**,**c**, -286290–286289 for **3a**,**b** contain the supplementary crystallographic data for this paper. These data can be obtained free of charge from The Cambridge Crystallographic Data Centre via www.ccdc.cam.ac.uk/data_request/cif.

Table 1. Crystal data and structure refinements for complexes **1a**, **2a**, **3a**, and others are listed as a footnote.

Compound	**1a**	**2a**	**3a**
formula	$C_{58}H_{34}CuEr_3N_2O_{24.50}$	$C_{34}H_{25}Cu_{1.5}O_{14.5}Yb$	$C_8H_4Cu_{0.5}Eu_{0.33}O_4$
F_w	1716.19	961.91	246.54
T [K]	293(2)	294(2)	293(2)
cryst system	triclinic	triclinic	rhombohedral
space group	$P\bar{1}$	$P\bar{1}$	$R\bar{3}c$
a [Å]	10.4762(7)	10.9774(13)	13.1118(11)
b [Å]	12.3802(9)	12.8338(16)	13.1118(11)
c [Å]	23.4254(16)	13.2340(16)	46.936(8)
α [°]	96.1230(10)	75.135(2)	90
β [°]	100.4500(10)	80.874(2)	90
γ [°]	111.8460(10)	69.436(2)	120
Z	2	2	36
V [Å^3]	2722.3(3)	1682.4(4)	6988.1(14)
ρ_{calcd} [mg m^{-3}]	2.094	1.899	2.109
R_1 and wR_2 $[I>2\sigma(I)]$[b,c]	0.0291, 0.0771	0.0339, 0.0776	0.0250, 0.0640
R_1 and wR_2 (all data)	0.0354, 0.0793	0.0455, 0.0895	0.0309, 0.0748

[a] **1b**: formula: $C_{58}H_{34}CuY_3N_2O_{24.50}$, M_r = 1481.14, T = 293(2) K, triclinic, $P\bar{1}$, a = 10.4762(7), b = 12.3802(9), c = 23.4254(16) Å, α = 96.1230(10), β = 100.4500(10), γ = 111.8460(10)°, V = 2722.3(3) Å^3, Z = 2, ρ_{calcd} = 1.807 g m^{-3}, the final R_1 = 0.0271, wR_2 = 0.0636; **1c**: formula: $C_{58}H_{34}CuEu_3N_2O_{24.50}$, M_r = 1679.30, T = 293(2) K, triclinic, $P\bar{1}$, a = 10.5478(5), b = 12.5171(5), c = 23.5260(10) Å, α = 95.6350(10), β = 100.8520(10), γ = 111.8670(10)°, V = 2782.4(2) Å^3, Z = 2, ρ_{calcd} = 2.004 g m^{-3}, the final R_1 = 0.0249, wR_2 = 0.0645; **2b**: formula: $C_{68}H_{50}Cu_3Gd_2N_4O_{29}$, M_r = 1892.24, T = 294(2) K, triclinic, $P\bar{1}$, a = 11.0119(15), b = 12.8729(19), c = 13.295(2) Å, α = 75.334(2), β = 81.530(3), γ = 69.204(2)°, V = 1701.0(4) Å^3, Z = 1, ρ_{calcd} = 1.847 g m^{-3}, the final R_1 = 0.0399, wR_2 = 0.0817; **2c**: formula: $C_{34}H_{25}Cu_{1.5}O_{14.5}Tb$, M_r = 947.79, T = 273(2) K, triclinic, $P\bar{1}$, a = 10.9785(5), b = 12.8812(6), c = 13.2657(6) Å, α = 75.065(10), β = 81.251(10), γ = 69.467(10)°, V = 1693.51(13) Å^3, Z = 2, ρ_{calcd} = 1.859 g m^{-3}, the final R_1 = 0.0202, wR_2 = 0.0557; **3b**: formula: $C_8H_4Cu_{0.5}Gd_{0.33}O_4$, M_r = 248.30, T = 293(2) K, rhombohedral, $R\bar{3}c$, a = b = 13.1335(9), c = 46.919(6) Å, γ = 120°, V = 7008.7(11) Å^3, Z = 36, ρ_{calcd} = 2.118 g m^{-3}, the final R_1 = 0.0226, wR_2 = 0.0627. [b] $R_1 = \Sigma||F_o|-|F_c||/\Sigma|F_o|$. [c] $wR_2 = \Sigma[w(F_o^2-F_c^2)^2]/\Sigma[w(F_o^2)^2]^{1/2}$.

Table 2. Selected bond lengths [Å] and angles [°] for **1a**, **2a**, **3a**.

1a		**2a**		**3a**	
Er2−O15#3	2.227(3)	Yb1−O5	2.228(4)	Eu1−O1	2.327(3)
Er2−O21	2.280(3)	Yb1−O4#1	2.245(4)	Eu1−O3#3	2.474(3)
Er2−O20	2.289(4)	Yb1−O12#2	2.252(4)	Eu1−O4#3	2.548(3)
Er2−O22#4	2.291(3)	Yb1−O9	2.330(4)	Cu1−O2#6	1.917(3)
Er2−O2#2	2.315(3)	Yb1−O8#3	2.349(4)	Cu1−O4#3	1.964(3)
Er2−O16#2	2.352(4)	Yb1−O1	2.379(4)	O1-Eu1-O1#1	82.51(10)
Er2−O24#1	2.393(4)	Yb1−O2	2.398(4)	O1-Eu1-O3#3	123.91(9)###
Cu1−O4	1.943(4)	Yb1−O7#3	2.445(4)	O1-Eu1-O4#4	148.54(9)
Cu1−N1	1.999(4)	Cu1−O3#1	1.930(4)	O3#5-Eu1-O4#4	128.20(10)
Cu1−O8#6	2.341(4)	Cu1−N1	1.995(5)	O2#6-Cu1-O2	180.0(2)
O4-Cu1-N2	91.51(18)	Cu2−O6	1.962(4)	O2#6-Cu1-O4#3	90.40(11)
N1-Cu1-N2	80.82(19)	Cu2−O11#2	1.966(4)	Cu1#7-O4-Eu1#8	114.02(11)
O4-Cu1-O8#	102.72(14)	O10-Cu1-N1	93.4(2)		
Er2#7-O2-Er1#7	110.49(13)	N2-Cu1-N1	81.7(2)		
Er1-O14-Er3	115.13(13)	O6#4-Cu2-O6	179.998(1)		
Cu1#6-O8-Er3#6	108.91(13)	O6#4-Cu2-O11#5	90.36(16)		

Symmetry codes: **1a**: #1: $-x+2$, $-y+2$, $-z+1$; #2: x, $y+1$, z; #3: $-x+1$, $-y+1$, $-z+1$; #4: $-x+1$, $-y+2$, $-z+1$; #5: $x+1$, y, z; #6: $-x+1$, $-y+1$, $-z$; #7: x, $y-1$, z; #8: $x-1$, y, z; **2a**: #1: $-x+2$, $-y+1$, $-z+1$; #2: $-x+1$, $-y+2$, $-z+1$; #3: $-x+2$, $-y+2$, $-z$; #4: $-x+2$, $-y+2$, $-z+1$; #5: $x+1$, y, z; #6: $x-1$, y, z; **3a**: #1: $-y+1$, $x-y+1$, z; #2: $-x+y$, $-x+1$, z; #3: $-y+^5/_3$, $-x+^4/_3$, $z-^1/_6$; #4: $-x+y-^1/_3$, $y-^2/_3$, $z-^1/_6$; #5: $x-^1/_3$, $x-y+^4/_3$, $z-^1/_6$; #6: $-x+1$, $-y+2$, $-z$; #7: $y-^2/_3$, $x+^2/_3$, $-z+^1/_6$; #8: $-y+^4/_3$, $-x+^5/_3$, $z+^1/_6$.

Acknowledgements

This work was supported by the National Natural Science Foundation of China under Project 50572040.

[1] a) H. B. Kagan, *Chem. Rev.* **2002**, *102*, 1805; b) C. E. Plecnik, S. Liu, S. G. Shore, *Acc. Chem. Res.* **2003**, *36*, 499; c) M. S. Wickleder, *Chem. Rev.* **2002**, *102*, 2011; d) J. Kido, Y. Okamoto, *Chem. Rev.* **2002**, *102*, 2357; e) J. R. Lombardi, B. Davis, *Chem. Rev.* **2002**, *102*, 2431; f) H. Tsukube, S. Shinoda, *Chem. Rev.* **2002**, *102*, 2389; g) Y. F. Zhou, M. C. Hong, X. T. Wu, *Chem. Commun.* **2006**, 135; h) J. C. G. Bünzli, *Acc. Chem. Res.* **2006**, *39*, 53; i) L. J. Barbour, *Chem. Commun.* **2006**, 1163; j) C. J. Kepert, *Chem. Commun.* **2006**, 695; k) C. N. R. Rao, S. Natarajan, R. Vaidhyanathan, *Angew. Chem.* **2004**, *116*, 1490; *Angew. Chem. Int. Ed.* **2004**, *43*, 1466.

[2] a) S. Osa, T. Kido, N. Matsumoto, N. Re, A. Pochaba, J. Mrozinski, *J. Am. Chem. Soc.* **2004**, *126*, 420; b) C. M. Zaleski, E. C. Depperman, J. W. Kampf, M. L. Kirk, V. L. Pecoraro, *Angew. Chem.* **2004**, *116*, 4002; *Angew. Chem. Int. Ed.* **2004**, *43*, 3912; c) B. Zhao, X. Y. Chen, P. Cheng, D. Z. Liao, S. P. Yan, Z. H. Jiang, *J. Am. Chem. Soc.* **2004**, *126*, 15394; d) H. Z. Kou, Y. B. Jiang, *Cryst. Growth Des.* **2005**, *5*, 77.

[3] a) M. B. Zhang, J. Zhang, S. T. Zheng, G. Y. Yang, *Angew. Chem.* **2005**, *117*, 1409; *Angew. Chem. Int. Ed.* **2005**, *44*, 1385; b) J. W. Cheng, J. Zhang, S. T. Zheng, M. B. Zhang, G. Y. Yang, *Angew. Chem.* **2006**, *118*, 79; *Angew. Chem. Int. Ed.* **2006**, *45*, 73.

[4] a) M. Eddaoudi, D. B. Moler, H. Li, B. Chen, T. M. Reineke, M. O'Keeffe, O. M. Yaghi, *Acc.Chem. Res.* **2001**, *34*, 319; b) O. M. Yaghi, M. O'Keeffe, N. W. Ockwig, H. K. Chae, M. Eddaoudi, J. Kim, *Nature* **2003**, *423*, 705.

[5] H. Li, C. E. Davis, T. L. Groy, D. G. Kelley, O. M. Yaghi, *J. Am. Chem. Soc.* **1998**, *120*, 2186.

[6] X. Zheng, C. Sun, S. Lu, F. Liao, S. Gao, L. Jin, *Eur. J. Inorg. Chem.* **2004**, 3262.

[7] a) M. L. Kahn, C. Mathoniere, O. Kahn, *Inorg. Chem.* **1999**, *38*, 3692; b) A. Q. Wu, G. H. Guo, C. Yang, F. K. Zheng, X. Liu, G. C. Guo, J. S. Huang, Z. C. Dong, Y. Takano, *Eur. J. Inorg. Chem.* **2005**, 1947.

[8] a) R. L. Carlin, A. J. v. Duyneveldt, Magnetic Properties of Transition Metal Compounds, Springer, Heidelberg (Germany), **1977**; b) O. Kahn, Molecular Magnetism, Wiley-VCH, Weinheim (Germany), **1993**.

[9] A. L. Spek, PLATON, Amultipurose Crystallographic Tool, Utrecht University, Utrecht (The Netherlands), **2001**.

[10] a) G. M. Sheldrick, SHELXS97, Program for Crystal Structure Determination, University of Göttingen (Germany), **1997**; b) G. M. Sheldrick, SHELXL-97-2, Program for Crystal Structure Refinement, University of Göttingen (Germany), **1997**.

[11] a) P. Mahata, G. Sankar, G. Madras, S. Natarajan, *Chem. Commun.* **2005**, 5787; b) C. J. Kepert, *Chem. Commun.* **2006**, 695; c) L. J. Barbour, *Chem. Commun.* **2006**, 1163; d) Y. S. Tao, H. Kanoh, L. Abrams, K. Kaneko, *Chem. Rev.* **2006**, *106*, 896.

Received: August 31, 2006
Revised: December 5, 2006
Published online: March 20, 2007

